Near-threshold fatigue propagation of physically through-thickness short and long cracks in a low alloy steel

Tuan Hiep Pham, Van-Xuan Tran, Gaëlle Chretien, Catherine Gardin, Jean Petit, Christine Sarrazin-Baudoux

Near-threshold fatigue propagation of physically through-thickness short and long cracks in a low alloy steel

Article *in* Journal of Materials Science · September 2014

Impact Factor: 2.37 · DOI: 10.1007/s10853-014-8582-8

Near-threshold fatigue propagation of physically through-thickness short and long cracks in a low alloy steel

Tuan-Hiep Pham, Van-Xuan Tran, Gaëlle Chretien, Catherine Gardin, Christine Sarrazin-Baudoux & Jean Petit

Journal of Materials Science
Full Set - Includes `Journal of Materials Science Letters'

ISSN 0022-2461

J Mater Sci
DOI 10.1007/s10853-014-8582-8

Springer

J Mater Sci
DOI 10.1007/s10853-014-8582-8

Near-threshold fatigue propagation of physically through-thickness short and long cracks in a low alloy steel

Tuan-Hiep Pham · Van-Xuan Tran · Gaëlle Chretien · Catherine Gardin · Christine Sarrazin-Baudoux · Jean Petit

Received: 24 June 2014 / Accepted: 31 August 2014

Abstract In this paper, the near-threshold fatigue behavior of physically through-thickness short cracks and of long cracks in a low alloy steel is investigated by experiments in ambient air. Physically through-thickness short fatigue cracks are created by gradually removing the plastic wake of long cracks in compact tension specimens. The crack closure is systematically measured using the compliance variation technique with numerical data acquisition and filtering for accurate detection of the stress intensity factor (SIF) at the crack opening. Based on the experimental results, the nominal threshold SIF range is shown to be dependent on the crack length and the characteristic of the crack wake which is strongly dependent on the loading history. The effective threshold SIF range and the relation between the crack propagation rate and the effective SIF range after the crack closure correction are shown to be independent on crack length and loading history. The shielding effect of the crack closure is shown to be related to the wake length and load history. The effective threshold SIF range and the relationship between the crack growth rate and the effective SIF range appear to be unique for this material in ambient air. These properties can be considered as specific fatigue properties of the couple material/ambient air environment.

T.-H. Pham · V.-X. Tran
Département Analyse Mécanique et Acoustique, EDF R&D, 92141 Clamart, France

T.-H. Pham · V.-X. Tran (✉)
Laboratoire de Mécanique des Structures Industrielles Durables, UMR CNRS-EDF-CEA 2832, 1 Av. du Général de Gaulle, 92141 Clamart, France
e-mail: van-xuan.tran@edf.fr

G. Chretien · C. Gardin · C. Sarrazin-Baudoux · J. Petit
Institut P', CNRS - Université de Poitiers–ENSMA, UPR 3346, SP2MI - Téléport 2, 1 avenue Clément Ader, BP 40109, 86961 Futuroscope Chasseneuil Cedex, France

Introduction

The ability to define the conditions under which cracks or defects are effectively non-propagating is a powerful mean for design and failure analysis. The threshold stress intensity factor (SIF) range, ΔK_{th}, was initially assumed to be a material parameter [1]. Using the concept of effective SIF range, ΔK^{eff}, initially defined by Elber [2], the concept of effective fatigue crack propagation is assumed to be representative for the intrinsic material properties [4]. Recently, the interest in the near-threshold fatigue crack growth and in the threshold concept has been accentuated by the problem of short fatigue cracks [5–15].

Current practice of characterizing fatigue crack growth based on the fracture mechanics primarily relies on fatigue tests for long cracks of which the length is typically of several millimeters. However, the design of numerous fatigue-critical engineering components requires understanding of the propagation of cracks of significantly smaller dimensions. Since the initial work of Pearson [5], many authors [7–24] have used continuum approaches to demonstrate that the growth rates of the small cracks can be significantly greater than those of the long cracks under the same nominal applied driving force. In addition, short fatigue cracks have been shown to propagate even at an applied SIF range smaller than the threshold SIF range determined with the long cracks, and to exhibit higher growth rates which were related to the lack of the crack closure [8, 10, 11, 13, 19–21]. In contrast, the high levels of crack closure which are often responsible for the low crack growth rates and crack arrest [1, 3, 24] are generally prevailed in the near-

Published online: 11 September 2014

threshold domain of long cracks. Consequently, the direct application of the experimental fatigue data obtained from specimens with the long cracks to design against the failure of components containing short flaws can, therefore, lead to dangerous overestimation of the fatigue lives [5, 9, 12, 21, 22]. The research in this area leads to awareness of the apparently anomalous behavior of small/short fatigue cracks [5–32]. Based on the basis of fracture mechanics principles, the long fatigue crack propagation can be predicted upon the concept of similitude [33]. The small crack problem can essentially be therefore considered as an inapplicability of the fracture mechanics parameters to uniquely characterize the growth of fatigue cracks independent of the crack size [8, 9, 26]. According to Suresh and Ritchie [9], different scales for crack size dependence can be considered. They suggested that short cracks can be broadly classified as: (i) cracks whose size is comparable to the scale of the characteristic microstructural dimension are referred as microstructurally small cracks; (ii) cracks for which the near-tip plasticity is comparable to the crack size are referred as mechanically small cracks; (iii) cracks whose size are significantly larger than the characteristic microstructural dimension and the scale of the local plasticity are referred as physically short cracks.

The present study focuses on the characterization of the near-threshold propagation of 2D physically through-thickness short cracks with an initial depth larger than 4 times the average grain size and only short in one dimension (crack depth). Such cracks are relevant to the third type of this small crack classification. The length of these fatigue cracks, typically of the order of 0.2–2.0 mm in length, is significantly longer than both the scale of the microstructure (grains size of 50 μm in the studied alloy) and the size of the near-tip yielding zone. This confirms the applicability of the linear elastic fracture mechanic concepts. Since crack closure mechanisms arise as a result of premature contact between the crack faces [2], and since, by definition, a short crack has a limited wake [2, 3], crack closure effects are generally less pronounced for a short crack propagating in a smooth specimen or ahead of a notch tip. Clear illustration of closure-induced difference between the long and short fatigue cracks can be found in the literature [10, 12–17, 23, 24, 34, 35]. Numerical simulation of the plasticity-induced closure for short crack has been recently investigated [35, 36] with a detailed comparison of experimental and numerical approaches for a 304 stainless steel.

The present study has been undertaken to investigate the influence of the crack length and loading history on the threshold for crack arrest in a low alloy steel. Physically through-thickness short cracks artificially obtained in CT specimens are tested in ambient air. The experimental results are then investigated. The role of crack closure is particularly taken into account.

Fig. 1 Material microstructure after etching with Nital 5 %

Specimens and experimental set-up

Material and specimen

The studied material is a low martensitic alloy steel. The microstructure revealed by etching process using a chemical solution of Nital 5 % (5 ml HNO_3 + 100 ml C_2H_5OH) appears to be isotropic with a grain size of about 50 μm as shown in Fig. 1. Fatigue crack growth tests are performed on CT40 specimens in accordance with the ASTM recommendations [37].

Creation of artificial 2D through-thickness short cracks in CT specimens

The creation of artificial physically through-thickness short crack consists of three steps, *pre-cracking, threshold test*, and *wake machining*. In the *pre-cracking step,* the crack is grown at an initial applied nominal SIF range $\Delta K_{initial}$ of 13 MPa.m$^{1/2}$ which is maintained constant from the crack initiation up to a crack length of about 2 mm. A *threshold test* is then performed using a load shedding procedure with load steps of 7 %. The crack length measurements are performed by mean of a traveling binocular microscope on both sides of the specimen. The reported crack length is the mean value of both measurements. The shedding procedure is programmed so as to reach the near-threshold domain for a crack length ratio *a/W* (crack length *a* to specimen width *W*) of about 0.5. This procedure provides optimized conditions for crack closure detection by the technique of compliance variation (see below).

In the *wake machining step,* the plastic wake of the initial long crack is gradually removed using an electro discharge machining (EDM) following the procedure schematically

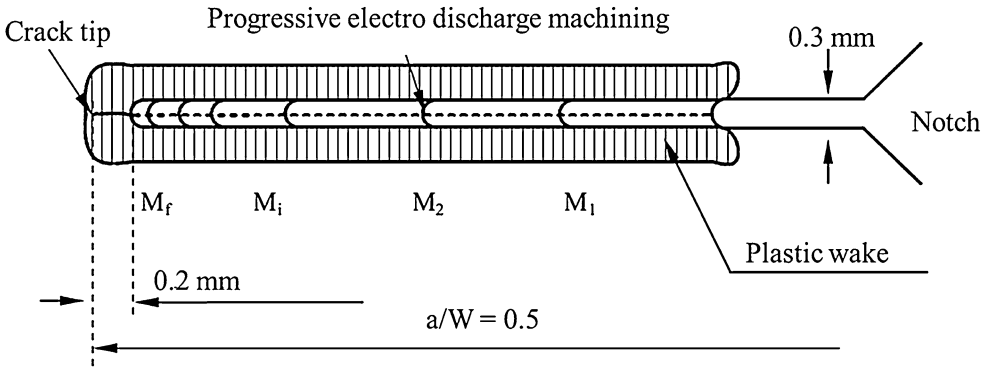

Fig. 2 A schematic plot of the machining process to create a short crack from a long pre-crack

illustrated in Fig. 2. The EDM wire is chosen with the smallest available diameter (0.25 mm) to minimize the change in the specimen geometry and to reduce at minimum size of the heat-affected zone near the crack tip. The loading history associated with the crack wake of the pre-crack is, therefore, mainly removed by the machining. A critical problem is to take care of the geometry of the pre-crack front. The EDM machining to create a remaining 2D short crack with lengths of about 0.2 mm on both sides is technically challenging to account for tilt and deflection of the crack plane and crack front misalignment. The machining is gradually conducted at least with three successive passes with a strict 3D control of the position of the crack tip with respect to the machined slot.

Testing conditions

Fatigue crack propagation tests are conducted in ambient air at room temperature on a standard 10 kN hydraulic INSTRON machine. The controlled parameters include frequency, load amplitude (ΔP), and mean load. For the artificial 2D through-thickness cracks, two types of tests, *threshold test* and *propagation test*, are conducted. For the *threshold test*, the conventional procedure used for pre-cracking cannot be straightly used. The objective was to get several successive threshold evaluations at increasing short crack lengths. Consequently, the threshold determination is made by these two steps. The threshold approach is started at a low SIF range $\Delta K = 6$ MPa.m$^{1/2}$. ΔK is then gradually decreased until the crack growth rate slower than 10^{-10} m/cycle. The *propagation tests* are performed under constant amplitude loading at a frequency set to be 35 Hz and a load ratio $R = 0.1$. The short crack length is measured with the traveling optical binocular microscope as described in the previous section.

Crack closure measurement

The compliance method initially proposed by Elber [2] is used to identify the opening SIF K_{op} and complemented by the differential technique as described in [35] and as schematically illustrated in Fig. 3. The tension load P is first recorded at a low frequency of 0.2 Hz as a function of the elastic strain δ measured by a strain gage (sticked on the back face of the specimen). The specimen compliance $\chi = \frac{\partial P}{\partial \delta}$ is extracted from the linear part of the P–δ diagram. The opening load P_{op} corresponds to the lower end of the linear part of this P–δ curve (Fig. 3a). To optimize the identification of P_{op}, differential Kikukawa compliance diagram P–δ' (schematically illustrated in Fig. 3b) is used with

$$\delta' = \delta - \frac{\mathrm{P}}{\chi}. \tag{1}$$

The value of P_{op} is determined at the level where the slope changes, and the opening SIF K_{op} is calculated as

$$K_{\mathrm{op}} = \frac{\Delta K}{P_{\max} - P_{\min}} P_{\mathrm{op}}. \tag{2}$$

A numerical data acquisition for P and δ is performed through a *computer interface*. The data processing is performed as detailed by Vor et al. [35].

Experimental results

Propagation of long cracks

The bi-logarithmic diagrams for the crack growth rate *da/dN* versus ΔK and versus ΔK^{eff} for a long crack growth using the procedure described above for the threshold test (descent data) and followed by a constant load amplitude test, i.e., at increasing ΔK (ascent data) up the final rupture, are plotted in Fig. 4. The ascent data appear very similar to the descent ones for the studied material. The correction for crack closure is accentuated when the threshold is approached. Note that for *da/dN* higher than 10^{-8} m/cycle (corresponding to $\Delta K > 13$ MPa.m$^{1/2}$), the shielding effect closure becomes negligible. The values of the nominal and effective SIF ranges under which the crack growth rate is

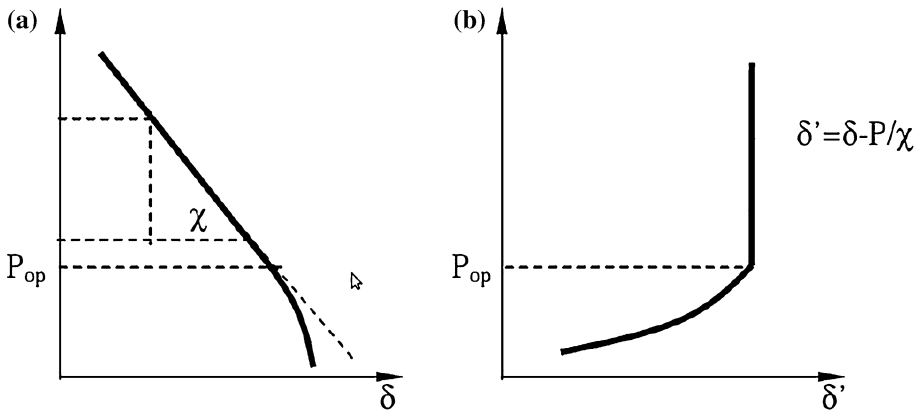

Fig. 3 Schematic plot of the complaisance method to measure the crack closure

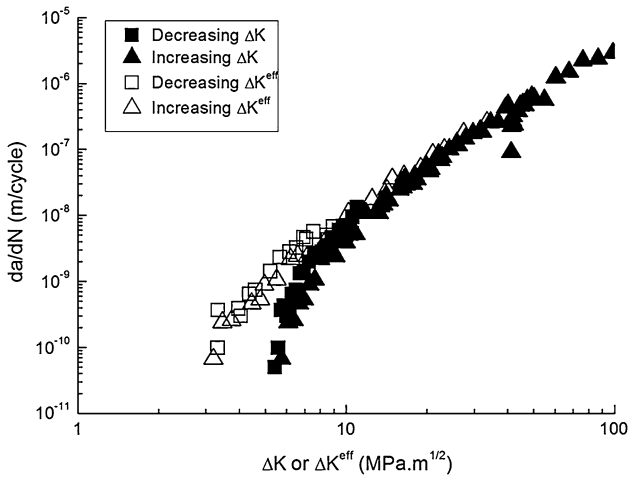

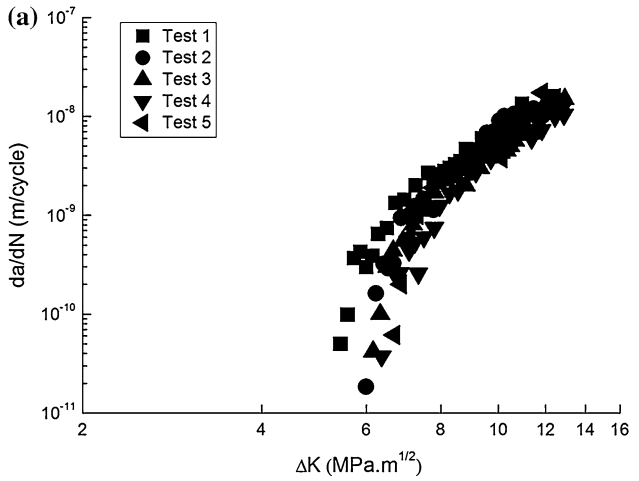

Fig. 4 Fatigue crack growth curves for the long crack using the nominal SIF range ΔK and the effective SIF range ΔK^{eff}

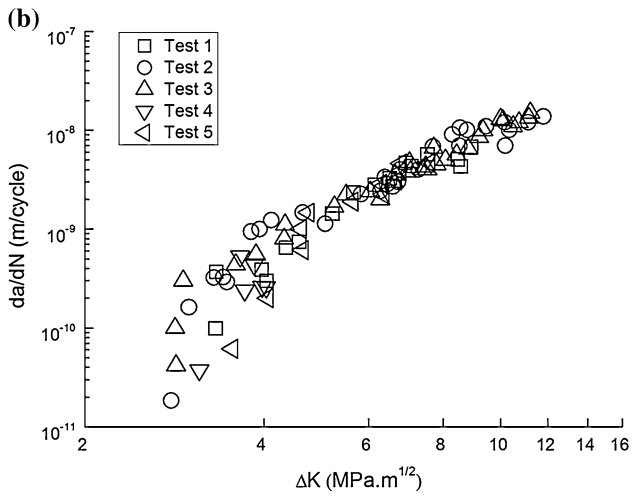

Fig. 5 Fatigue crack growth curves for the long crack using **a** the nominal SIF range ΔK and **b** the effective SIF range ΔK^{eff}

lower than 10^{-10} m/cycle are considered representative of the threshold ranges. These values are obtained as

$$\Delta K_{\text{th}}^{\text{lc}} \approx 5.5\,\text{MPa.m}^{1/2};\ \Delta K_{\text{th}}^{\text{eff,lc}} \approx 3.3\,\text{MPa.m}^{1/2}, \tag{3}$$

where the subscript "th" stands for "threshold" and the superscripts "lc" and "eff" stand for "long crack" and "effective", respectively.

For $\Delta K > 13$ MPa.m$^{1/2}$, i.e., in a domain which can be assimilated to the Paris' zone, the closure effect can be neglected, and the Paris' law can be written as

$$\frac{da}{dN} \approx 6.10^{-9}\left(\Delta K^{\text{eff}}\right)^{3.4} \approx 6.10^{-9}(\Delta K)^{3.4}. \tag{4}$$

The present study being concentrated on the evolution of crack closure with the crack length, in the following, the tests now here considered are performed at $\Delta K < 13$ MPa.m$^{1/2}$, i.e., when the shielding effect of crack closure becomes substantial. For the preparation of the five CT specimens used to create artificial 2D short cracks, the near-threshold fatigue crack propagation curves are plotted as functions of the nominal SIF range ΔK in Fig. 5a and of the effective SIF range ΔK_{eff} in Fig. 5b.

The five nominal propagation curves (Fig. 5a) are very close one from the others for *da/dN* higher than 5×10^{-9}

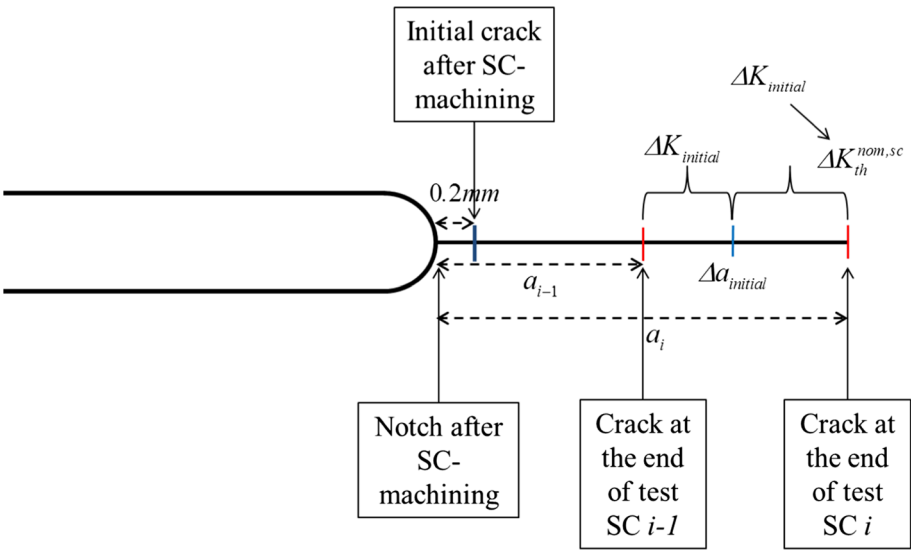

Fig. 6 A schematic plot of the tests conducted on the specimen with the short crack

Table 1 The testing conditions and experimental results of the 7 short crack tests with $\Delta K_{initial}^{nom} = 6\,MPa.m^{1/2}$

Test number	Initial crack length a_{i-1} (mm)	$\Delta K_{th}^{nom,sc}$ (MPa.m$^{1/2}$)	$\Delta K_{th}^{eff,sc}$ (MPa.m$^{1/2}$)	Final crack length a_i (mm)
1	0.23	3.88	3.68	0.46
2	0.46	4.16	3.70	0.67
3	0.67	4.21	3.28	0.86
4	0.86	4.04	3.63	1.23
5	1.23	4.18	3.60	1.51
6	1.51	4.18	3.34	1.74
7	1.74	4.18	3.43	1.93

m/cycle. As shown in the figure, in the near-threshold domain, i.e., *da/dN* lower than 5×10^{-9} m/cycle, a substantial scatter is observed. On one hand, the nominal threshold SIF for long crack ΔK_{th}^{lc} varies from 5.5 MPa.m$^{1/2}$ to 6.8 MPa.m$^{1/2}$ with an average value of 6.2 MPa.m$^{1/2}$. The difference of the measured ΔK_{th}^{lc} between one specimen and the others may be attributed to a different closure contribution for each specimen. In the other hand, the effective crack propagation curves (Fig. 5b) show a remarkable agreement for the data provided at growth rates higher than 3×10^{-10} m/cycle. As shown in the figure, in the very near-threshold domain, the five effective curves fall in a same scatter band. Thus, while the nominal threshold SIF range cannot be considered as a material property, the effective threshold gradually can be considered as a specific property of the studied alloy in air environment. The effective threshold SIF range can be evaluated as $\Delta K_{th}^{eff,lc} = 3.4 \pm 0.3$ MPa.m$^{1/2}$. Moreover, the effective crack propagation relationship *da/dN* versus ΔK^{eff} can be considered as a specific fatigue property of the couple material/ambient air environment.

Propagation of short cracks

A schematic of the procedure used for the threshold tests for artificial short cracks is shown in Fig. 6. Starting from an initial length on the specimen surface of 0.2 mm, seven successive threshold tests are conducted starting with the same initial nominal SIF range $\Delta K_{initial} = 6$ MPa.m$^{1/2}$ at $R = 0.1$ (see Table 1).

The corresponding near-threshold crack propagation curves for the short curves with increasing length and the corresponding effective curves after closure correction are presented in Fig. 7. The successive threshold SIF ranges are measured for crack lengths ranging from 0.46 to 1.93 mm. The values of the nominal and effective threshold SIF ranges are reported in Table 1. The first threshold SIF range at a length of 0.46 mm is slightly lower than the six following thresholds measured at lengths ranging from 0.67 upto 1.93 mm. The first threshold is measured at 3.9 MPa.m$^{1/2}$, and the six following ones are ranged at 4.1 ± 0.1 MPa.m$^{1/2}$. Note that these values are substantially lower than the threshold for the initial long cracks, i.e., $\Delta K_{th}^{lc} = 6.2 \pm 0.6\,MPa.m^{1/2}$ (see Fig. 8).

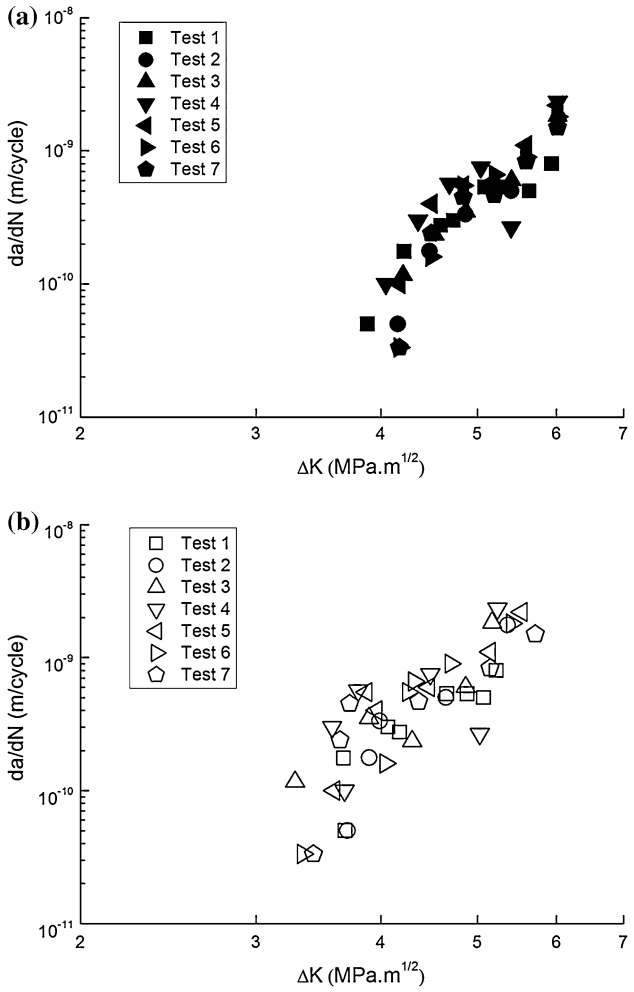

Fig. 7 7 short crack propagation tests with initial $\Delta K = 6$ MPa.m$^{1/2}$, **a** *da/dN* vs ΔK **b** *da/dN* vs ΔK^{eff}

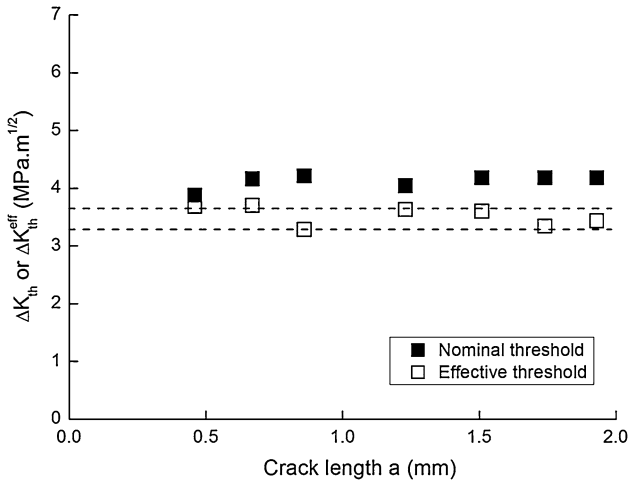

Fig. 8 Threshold SIF ranges as functions of the crack length obtained from seven tests for specimens with short crack with $\Delta K_{\text{initial}} = 6$ MPa.m$^{1/2}$

Based on the limited number of experimental results and with a substantial scatter, the effective propagation curves (Fig. 7) appear comparable, and the effective threshold can be established as $\Delta K_{\text{th}}^{\text{eff,sc}} = 3.5 \pm 0.2$ MPa.m$^{1/2}$ (the superscript "sc" stands for "short crack") independently on the crack length, this value being very similar to that of the effective threshold measured for the initial long cracks, i.e., $\Delta K_{\text{th}}^{\text{eff,lc}} = 3.4 \pm 0.3$ MPa.m$^{1/2}$. These results support a significant contribution of the crack closure shielding mechanism for the seven short cracks but which is much less marked than for the initial long cracks. It is also noticeable that except for the first threshold SIF range at 0.46 mm, the effective threshold does not vary with the short crack length in the used experimental conditions (initial ΔK range, ratio $R = 0.1$, shedding parameters). It comes out that, in spite of data scatter, the effective threshold SIF range appears to be, in any case, independent on the crack length and on the load history and thus can be confirmed as a specific property of the couple material/air environment.

Regarding the potential influence of the crack length, the absence of variation of the nominal threshold with the crack length for the seven tests run with the same initial ΔK, except a slightly lower threshold SIF range for the first at 0.46 mm, suggests that the closure may be located in the very first tenth of millimeter of the crack wake. This observation appears to be in contradiction with the results for the long cracks tested under other conditions, namely with a much higher initial ΔK range of 13 MPa.m$^{1/2}$. Finally, these results suggest that there may exist more complex mechanisms controlling the shielding effect of closure for the short cracks as well as for the long cracks for this particular material. Note also that these results are not in accordance with the short fatigue behavior reported in the previous studies for 304L stainless steel as in [36]. As reported in this reference, the nominal threshold SIF range generally increases when the length of the short crack increases up to a crack length for which the closure contribution becomes negligible (when it becomes independent on the crack length, i.e., when the crack is considered as a long one). A classical graphical description to relate this behavior has been initially proposed by Kitagawa and Takahashi [38]. The crack closure phenomenon being straightly related to the crack wake, an unknown effect of the load history can be expected, and thus additional tests are performed to try to answer this problem.

Five additional tests are then conducted on the same specimen as the one used for the previous series of seven thresholds for the progressively growing short cracks. It is noticed that the last threshold of this previous series corresponds to a crack having a length of 1.93 mm. This crack length, close to 2 mm, is generally a length expected for a crack to behave like a long crack. However, the closure SIF

Table 2 The testing conditions and experimental results of the short crack tests 8–12

Test number	Initial crack length a_{i-1} (mm)	$\Delta K_{initial}^{nom}$ (MPa.m$^{1/2}$)	$\Delta a_{initial}$ (mm)	$\Delta K_{th}^{nom,sc}$ (MPa.m$^{1/2}$)	$\Delta K_{th}^{eff,sc}$ (MPa.m$^{1/2}$)	Final crack length a_i (mm)
8	1.93	8	0.05	4.48	3.67	2.23
9	2.23	10	0.05	4.36	3.49	2.97
10	2.97	13	0.05	4.38	3.29	3.78
11	3.78	13	0.25	4.71	3.48	4.68
12	5.60	13	1.22	5.90	3.21	7.31

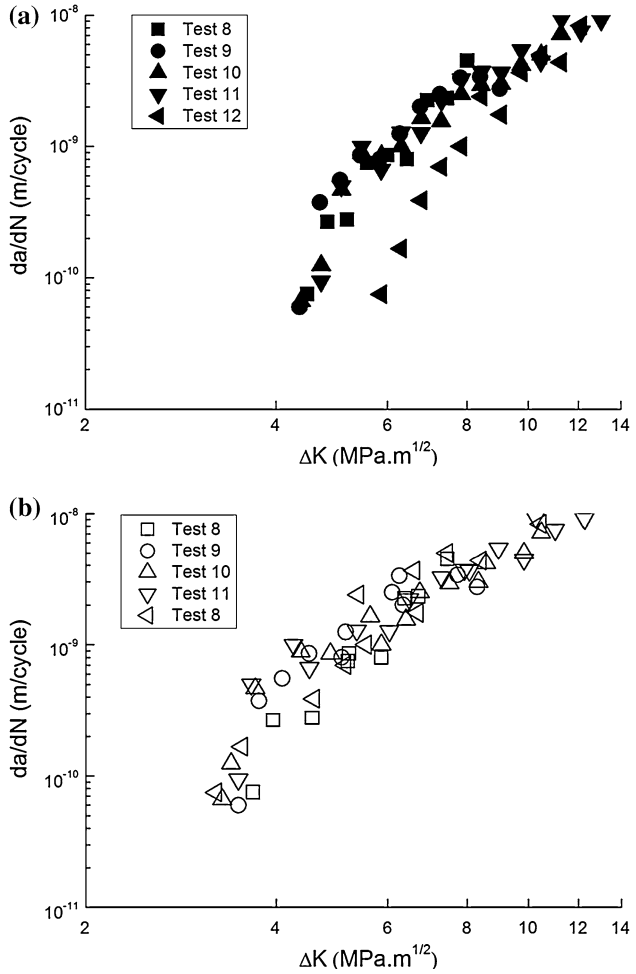

Fig. 9 5 short crack propagation tests with initial $\Delta K = 8$, 10, 13 MPa.m$^{1/2}$, **a** *da/dN* vs ΔK; **b** *da/dN* vs ΔK_{eff}

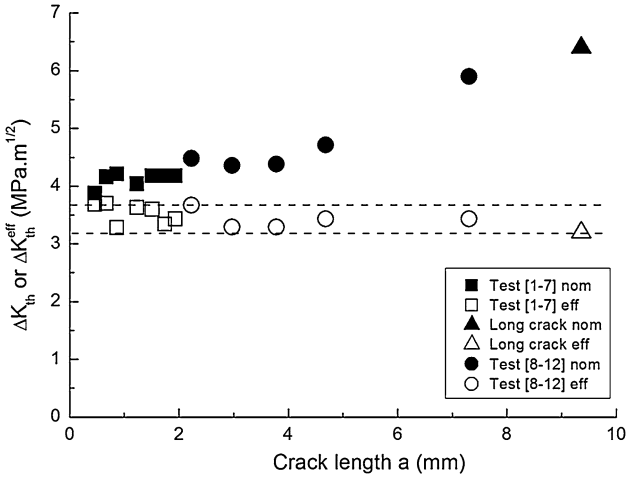

Fig. 10 Nominal and effective threshold SIF ranges as functions of the crack length with different $\Delta K_{initial}$ (*filled symbols* for nominal thresholds, *opened symbols* for effective thresholds)

K_{op} for the seventh test is much lower than for the long crack growth with an initial ΔK of 13 MPa.m$^{1/2}$ with a wake built at this level all along an initial precracking of 2 mm. Based on this consideration, the testing conditions for these five following tests referenced #8 to #12 given in Table 2, correspond to increased initial $\Delta K_{initial}$ levels. The propagation curves are plotted in Fig. 9. The evolution of the nominal and effective threshold ranges is plotted in Fig. 10. For the next three tests initiated at 8, 10, and 13 MPa.m$^{1/2}$ with a small initial crack growth step of 0.05 mm under the upper SIF range for each test, the threshold is poorly affected by the increase of the crack length and by the initial ΔK range. For tests #4 and #5 with the same initial amplitude range $\Delta K_{initial} = 13$ MPa.m$^{1/2}$, the initial crack growth step is conducted along a crack step of 0.25 and 1.2 mm, respectively. The following threshold SIF ranges are higher than the preceding ones, with a slight increase for the initial step of 0.25 mm, but much higher increase for the step of 1.22 mm, the nominal threshold SIF range becoming close to that measured for the long crack tests with an initial step of about 2 mm at the same SIF range $\Delta K_{initial} = 13$ MPa.m$^{1/2}$. For all these tests, the effective threshold SIF range is still at the same level, i.e., $\Delta K_{th}^{eff,lc} = 3.4 \pm 0.3$ MPa.m$^{1/2}$ whatever the crack length and the initial ΔK range. Consequently, the difference observed in the near-threshold behavior and in the threshold level in relation with the crack length and the initial ΔK levels is induced by the difference in the crack closure contribution. The results obtained with different conditions of propagation before the threshold procedure show that the closure contribution depends straightly on the wake history as well as in term of SIF level as on wake length.

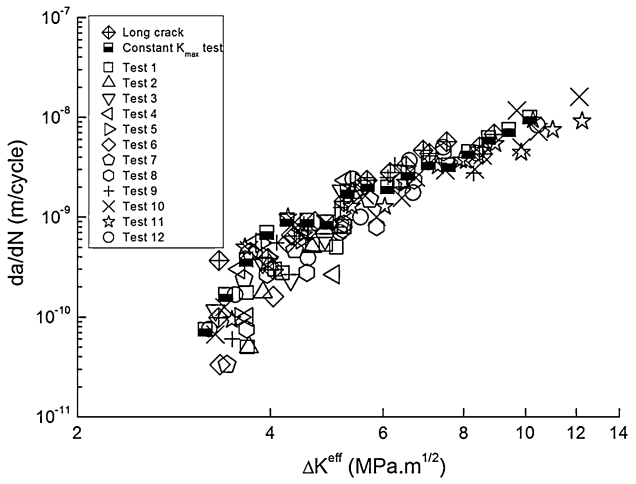

Fig. 11 Effective fatigue crack growth compared to the K_{max}-constant test

This wake history effect is not uniquely typical of short cracks as demonstrated by tests #10 to #12.

Discussion

The experiments conducted in this study in the near-threshold domain put in light a major role of the crack closure. However, the crack closure measurements performed in the very near-threshold area exhibit a substantial scatter. This leads to a difficulty to detect precisely the opening SIF level K_{op} even with sophisticated numerical signal analysis, especially for very short crack wake with very small amplitude of variation of the specimen compliance. To substantiate and validate the obtained results, a reference test is conducted in a loading condition avoiding crack closure and directly providing the effective propagation curve. For this test, the maximum SIF K_{max} is kept constant. The initial minimum SIF $K_{min,initial}$ is chosen to be larger than the value of K_{op} obtained from the previous tests. Then the nominal SIF range $\Delta K = K_{max} - K_{min}$ is decreased gradually with steps of 7 % by increasing K_{min}, which means at increasing R ratio, instead of decreasing ΔK range as done for the other tests at $R = 0.1$. Thus, all along this threshold test, the condition $K_{min,initial} > K_{op}$ is verified so that the closure effect is eliminated. The nominal and effective threshold values are nearly the same and measured as

$$\Delta K_{th}^{nom} \approx \Delta K_{th}^{eff} \approx 3.2\,\mathrm{MPa.m}^{1/2}. \quad (5)$$

The experimental results for this K_{max}-*constant* test are confronted to the effective long and short crack data after closure correction in Fig. 11. For growth rates higher than 3×10^{-9} m/cycle, all the results are very consistent with the existence of a unique effective relationship between the growth rate *da/dN* and the effective SIF range ΔK^{eff}. In the very near-threshold domain, even with the measurement scatter, the data provided after closure correction are all in agreement with the reference effective propagation provided by the K_{max}-*constant* test. Finally, the effective crack propagation is given by a unique relationship for all the cracks grown in the studied alloy whatever the crack length or the load history.

Regarding the so-called short crack effect, as noticed above, the first short crack threshold SIF range at a crack length of 0.46 mm with a test initiated at $\Delta K = 6\ \mathrm{MPa.m}^{1/2}$ is measured at $3.9\ \mathrm{MPa.m}^{1/2}$. This value is slightly lower than the average value provided by the six following threshold SIF ranges for the short cracks, i.e., $\Delta K_{th}^{sc} = 4.1 \pm 0.1\ \mathrm{MPa.m}^{1/2}$ (for crack length ranging from 0.67 to 1.93 mm). This suggests that, in this material, the short crack effect may be very small and concentrated in the five to six first tenths of mm of the crack length. Finally, the most marked effect of closure is related to the crack wake history. This appears to be somehow specific of this material since similar observation has not been reported in the literature. Further exploration is needed to evaluate and model the influence of the various factors which can affect the crack wake.

Conclusion

The following conclusions can be drawn from this study of the near-threshold fatigue propagation of physically through-thickness short and long cracks in a low alloy steel:

- The faster crack growth rates observed for 2D physically short cracks artificially obtained from machining the wake of long precracks are explained in term of a lower contribution of crack closure as detected using the variation compliance technique with numerical data analysis to optimize the sensitivity of the technique.
- The shielding effect of crack closure is shown to be related to the wake length and to the load history during the building of the crack wake.
- The influence of the crack wake is observed not only for short cracks but also for long cracks.
- The effective threshold SIF range and the crack propagation relationship between *da/dN* and the effective SIF range are unique for this material in ambient air. They may be considered as intrinsic properties of the couple alloy/air environment. The further work in different environments will be investigated to confirm this purpose.

Acknowledgement The financial support of this work by DALIA/CAMELIA project from EDF R&D is greatly appreciated.

References

1. Davidson D, Suresh S (1984) Fatigue crack growth threshold concept. TMS AIME Pub, Warendale
2. Elber W (1970) Fatigue crack closure under cyclic tension. Eng Fract Mech 2:37–45
3. Newman Jr JC, Elber W (1988) Mechanics of fatigue crack closure, ASTM STP 982, American Society for Testing and Materials, pub., Philadelphia, USA
4. McClung RC, Newman JR JC (1999) Advances in fatigue crack closure measurement and analysis, volume 2. ASTM STP 1343, American Society for Testing and Materials pub, Philadelphia, USA
5. Pearson S (1975) Initiation of fatigue cracks in commercial aluminum alloys and the subsequent propagation of very short cracks. Eng Fract Mech 7:235–247
6. Healy J, Bushby AJ, Mai YW, Mukhopadhyay AK (1997) Cyclic fatigue of long and short cracks in alumina. J Mater Sci 32(3):741–747. doi:10.1023/A:1018556322981
7. Fett T, Martin G, Munz D, Thun G (1991) Determination of da/dN-$\Delta K_{\mathbf{I}}$ curves for small cracks in alumina in alternating bending tests. J Mater Sci 26(12):3320–3328. doi:10.1007/BF01124680
8. Miller KJ (1982) The short crack problem. Fatigue Eng Mater Struct 5:223–232
9. Suresh S, Ritchie RO (1984) Propagation of short fatigue cracks. Int Met Rev 29:445–476
10. Zeghloul A, Petit J (1985) Environmental sensitivity of small crack growth in 7075 aluminium alloy. Fatigue Fract Eng Mater Struct 8:341–348
11. Lankford J, Ritchie RO (1986) Small Fatigue Cracks. TMS AIME publication, Warendale
12. Pineau A (1986) Short fatigue crack behaviour in relation to three dimensional aspects and crack closure effect. Lankford J and Ritchie RO eds TMS AIME pub Warrendale, pp. 191–209
13. Ritchie RO, Yu W (1986) Short crack effecting fatigue: a consequence of crack tip shielding. Small fatigue cracks. Lankford J and Ritchie RO editors TMS AIME pub Warrendale, pp. 167–189
14. Venkateswara Rao KT, Yu W, Ritchie RO (1986) Scr Metall. 20:1459–1464
15. McClung RC, Sehitoglu, H (1988) Closure behavior of small cracks under high strain fatigue histories. In: J. C. Newman Jr. and W. Elber (eds), Mechanics of Fatigue Crack closure, vol. 982. ASTM STP, pp. 279–299
16. Zeghloul A, Petit J (1989) Influence de l'environnement sur la propagation des fissures courtes et longues dans un alliage léger type 7075. Revue de Physique 24:893–904
17. Zeghloul A, Petit J (1989) Influence de l'environnement et de la microstructure sur la propagation en fatigue des fissures courtes tridimensionnelles. Revue de Physique Appliquée 24:905–913
18. Petit J, Zeghloul A (1990) Environmental and Microstructural Influence on Fatigue Propagation of Small Surface Cracks. In: Lisagor WB, Crooker TW and Leis BN eds, Environmentally Assisted Cracking: Science and Engineering, Vol. ASTM STP 1049, pp. 334–346
19. Miller KJ, De los Rios ER (1992) Short fatigue cracks. ESIS 13. Mechanical Engineering Publication, London
20. Petit J, Mendez J, Berata W, Legendre L, Muller C (1992) Influence of environment on the propagation of short and long cracks in a titanium alloy. In: Miller KJ and de Los Rios ER (eds), Short fatigue cracks, ESIS 13, London, MEP pub, pp. 235–250
21. Newman JC Jr (1998) The merging of fatigue and fracture mechanics concepts: a historical perspective. Prog Aerosp Sci 34:347–390
22. Ravichandran KS, Ritchie RO, Murakami Y (1999) Small fatigue cracks: mechanics and mechanisms. Engng Foundation Publication, Oxford, UK
23. Petit J (1999) Influence of environment on small fatigue crack growth. In: Small fatigue cracks, mechanics, mechanisms and applications, Ravichandran KS, Ritchie RO, Murakami Y (eds), Elsevier Pub., Amsterdam, pp. 167–178
24. Petit J (1984) Some aspects of near threshold fatigue crack growth: microstructural and environmental effects. In: Davidson D, Suresh S (eds) Fatigue crack growth threshold concepts. TMS, AIME, Philadelphia, pp 3–24
25. Zhang XP, Wang CH, Ye L, Mai Y-W (2005) A study of the crack wake closure/opening behavior of short fatigue cracks and its influence on crack growth. Mater Sci Eng A406:195–204
26. Christ HJ, Duber O, Floer W, Krupp U, Fritzen CP, Kunkler B, Schick A (2006) Microstructural effect on short fatigue crack propagation and their modeling. Fracture of nano and engineering materials and structures, Proceedings of the 16th European Conference of Fracture, E E Gdouos ed, Springer pub, Netherlands pp. 9–863
27. Mann T, Härkegard G, Stärk K (2007) Short fatigue crack growth in aluminum alloy 6082-T6. Int J Fatigue 29:1820–1826
28. McEvily AJ, Ishihara S, Endo M, Sakai H, Matsunaga H (2007) On one- and two-parameter analyses of short fatigue crack growth. Int J Fatigue 29:2237–2245
29. Chang H, Han EH, Wang JQ, Ke W (2009) Acoustic emission study of fatigue crack closure of physical short and long cracks for aluminum alloy LY12CZ. Int. J Fatigue 31:403–407
30. Verreman Y, Limodin N (2008) Fatigue notch factor and short crack propagation. Eng Fract Mech 75:1320–1335
31. Hansson P, Melin S (2010) Influence from geometrical features on the growth rate of a micro-structurally short fatigue crack. Eng Fract Mech 77:1907–1913
32. Santus C, Taylor D (2009) Physically short crack propagation in metals during high cycle fatigue. Int J Fatigue 31:1356–1365
33. Rice JR, Paris PC, Merkle JG (1973) In: Progress in flaw growth and fracture toughness testing. ASTM STP 536, American Society for Testing and Materials pp. 231–245
34. Zhang JZ, Zhang JZ, Du YS (2001) Elastic-plastic finite element analysis and experimental study of short and long fatigue crack growth. Eng Fract Mech 68:1591–1605
35. Vor K, Gardin C, Sarrazin-Baudoux C, Petit J (2013) Wake length and loading history effects on crack closure of through-thickness long and short cracks in 304L: Part I—Experiments. Eng Fract Mech 2013(99):266–277
36. Vor K, Gardin C, Sarrazin-Baudoux C, Petit J (2013) Wake length and loading history effects on crack closure of through-thickness long and short cracks in 304L: Part II—3D numerical simulation. Eng Fract Mech 99:306–323
37. ASTM E647-00 (2000) Standard test method for measurement of fatigue crack growth rates, ASTM International
38. Kitagawa H, Takahashi S (1976) Applicability of fracture mechanics to very small cracks on the crack in the early stage, Second International Conference on Mechanical Behaviour of Material